Title

Potent and Selective EphA4 Agonists for the Treatment of ALS

Journal

Cell Chemical Biology, 24(3)

ISSN

2451-9456

Authors

Wu, Bainan

De, Surya K

Kulinich, Anna

et al.

Publication Date

2017-03-01

DOI

10.1016/j.chembiol.2017.01.006

Peer reviewed

Published in final edited form as:

Cell Chem Biol. 2017 March 16; 24(3): 293–305. doi:10.1016/j.chembiol.2017.01.006.

Potent and selective EphA4 agonists for the treatment of ALS

Bainan Wu[1], **Surya K. De**[2], **Anna Kulinich**[2], **Ahmed F. Salem**[2], **Jordan Koeppen**[2], **Rengang Wang**[1,3], **Elisa Barile**[2], **Si Wang**[1], **Dongxiang Zhang**[1], **Iryna Ethell**[2], and **Maurizio Pellecchia**[2,*]

[1]Sanford-Burnham-Prebys Medical Discovery Institute, 10901 North Torrey Pines Rd. La Jolla, CA 92037, USA

[2]Division of Biomedical Sciences, School of Medicine, University of California Riverside, 900 University Avenue, Riverside, CA 92521, USA

[3]Brain Development, University of California San Diego, San Diego, CA 92090

Abstract

Amyotrophic lateral sclerosis (ALS) is a progressive degenerative disease that affects motor neurons. Recent studies identified the receptor tyrosine kinase EphA4 as a disease-modifying gene, critical for the progression of motor neuron degeneration. We report on the design and characterization of a family of EphA4 targeting agents that bind to its ligand binding domain with nanomolar affinity. The molecules exhibit excellent selectivity and display efficacy in a SOD1 mutant mouse model of ALS. Interestingly, the molecules appear to act as agonists for the receptor in certain surrogate cellular assays. While the exact mechanism(s) that are responsible for the therapeutic effect of the new agonists remain to be elucidated, we believe that the described agent represents both an invaluable pharmacological tool to further decipher the role of the EphA4 in ALS and potentially other human diseases, and a significant stepping stone for the development of novel treatments.

eTOC blurb

[*]Lead contact and corresponding author: Maurizio Pellecchia, phone number: (951) 827-7829; maurizio.pellecchia@ucr.edu.

Author contributions: MP directed research, designed and conceived the compounds listed, coordinated testing of the molecules, interpreted data and results, and wrote the manuscript. MP also performed all modeling studies and prepared several of the Figures. BW prepared proteins and mutants, developed the FP assay, tested compounds by NMR and prepared several of the Figures and wrote an initial draft of the manuscript. SKD synthesized compounds and prepared Fig. S6. SW helped with analytical studies. AFS prepared the stable cell line and performed the experiments reported in Fig. S7. EB helped assessing compounds' selectivity, including binding affinities for the EphA3 receptor and conducted stability in plasma (Fig. S4). JK and AK under the supervision of IE performed and analyzed the data reported in Figs. 4 and 5A-G. RW under the supervision of DZ performed and analyzed the *in vivo* efficacy studies reported in Fig. 5H,I.

Competing interests: SBPMDI has licensed the reported compounds and derivatives, including other derivatives not disclosed in this manuscript and prophetic compounds, to Iron Horse Therapeutics, Inc. of San Diego (CA) for their development into novel ALS therapies.

Data and materials availability: Small amounts of 123C4 can be made available for research purposes through a standard MTA.

Wu et al. report on the design and characterization of a novel, *bona fide*, potent and selective ligand targeting the EphA4 receptor that is very efficacious in delaying the progression of ALS in mice models.

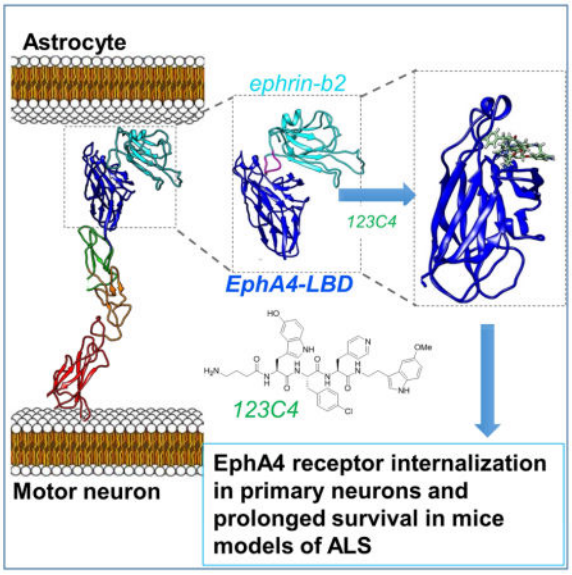

Introduction

Amyotrophic lateral sclerosis (ALS) is a progressive degenerative disease that affects motor neurons. Mutations in SOD1 (superoxide dismutase 1) and in hexanucleotide repeats in the non-coding region of *C9orf72*, seem the most prevalent in those affected by the disease (Rosen et al., 1993) (DeJesus-Hernandez et al., 2011). Despite tremendous efforts aimed at identifying contributing factors for ALS, the mechanisms underlying motor neuron death have not yet been fully elucidated and consequently no effective treatment is currently available for ALS, in spite of several clinical trials based on drugs from animal studies, which have been conducted and ultimately failed. Among the possible reasons for such failures is the lack of a proper drug target.

In this regard, a zebrafish model for ALS was developed by expression of mutant-SOD1 in embryos that resulted in shorter and aberrantly branched axons of motor neurons (Lemmens et al., 2007). This model has been used to investigate possible disease-modifying genes, resulting in the identification of Rtk2 (the zebrafish equivalent of human EphA4) as a critical gene for the onset and progression of the disease. Rtk2 knockdown in mutant-SOD1 zebrafish rescued the motor axonopathy induced by three different SOD1 mutations (A4V, G93A, G37R), without affecting axonal length (Van Hoecke et al., 2012). Pharmacological inhibition of the EphA4 with an EphA4-blocking peptide (Murai et al., 2003) via an intra-cerebro-ventricular administration, enhanced recovery and axonal sprouting in models of spinal cord injury possibly through the suppression of reactive astrogliosis (Goldshmit et al., 2004), and it prolonged survival in ALS rats overexpressing human mutant SOD1(G93A) (Van Hoecke et al., 2012). Moreover, in humans with ALS, EphA4 expression correlates

inversely with disease onset and overall survival, while loss-of-function mutations in EphA4 are associated with long survival (Van Hoecke et al., 2012).

These studies clearly suggest that the EphA4 is a potential target for ALS and that targeting its ligand–binding domain may provide a possible avenue to novel and effective therapeutics. Based on these premises, we report here on the design, synthesis and characterization of a novel family of EphA4 agents targeting its ligand-binding domain. The molecules exhibit nanomolar affinity for the EphA4 receptor with > 10 fold selectivity over the closest receptor of the family (EphA3), are brain penetrant and show efficacy in a SOD1 mutant mouse model of ALS. Intriguingly, the agents act as EphA4 agonists in primary cortical neuron, suggesting that alternative mechanisms correlating EphA4 expression with disease progression may involve reverse signaling perhaps on ephrin-B2 expressing reactive astrocytes. While the exact mechanism(s) that are responsible for the therapeutic efficacy of our agents remains to be elucidated, we are confident that our molecules represent useful and much needed *bona fide* pharmacological tools for deciphering the role of EphA4 signaling in ALS and potentially other human diseases, including Alzheimer disease (AD) (Fu et al., 2014), spinal cord injury (Spanevello et al., 2013), brain injury (Frugier et al., 2012; Hanell et al., 2012), and some type of cancers (Fukai et al., 2008; Iiizumi et al., 2006; Miyazaki et al., 2013; Oshima et al., 2008). Collectively our agents and related data form the basis for the development of novel therapeutics.

Results

Design, synthesis, and characterization of novel EphA4-LBD ligands

We recently reported on an innovative nuclear magnetic resonance (NMR)-guided approach in which positional scanning libraries of peptide-mimetics are tested using highly sensitive NMR screening methods (Wu et al., 2013). The approach was preliminarily tested against the ligand binding domain of the EphA4 receptor, resulting in the low micromolar compound 22 (Table 1). Structure-activity relationships studies were further conducted on the core structure of compound 22, exploring preferences of substituents in different positions of the molecule (Table 1). Two orthogonal assays were used to further quantify the binding affinities. As first assay, we developed a displacement fluorescence polarization assay (FPA) using a fluorescently labeled EphA4-LBD binding peptide of sequence KYLPYWPVLSSL (KYL in short), previously reported to binding specifically to the EphA4-LBD with low micro-molar affinities (Murai et al., 2003). In addition, we further measured the direct dissociation constant between test molecules and EphA4–LBD using isothermal titration calorimetry (ITC). The latter method is also useful to determine the detailed thermodynamics of binding. Starting from compound 22, we sought to modify its N- and C- terminal ends to increase its binding affinity for EphA4-LBD. Moreover, our working hypothesis was that replacement of both termini with non-natural amino acids could result in increased resistance to proteases *in vivo* and overall improved *drug-likeness* of the resulting peptide mimetic, based on our recent experience with other related systems (Wu et al., 2015b). Several structure-activity relationships emerged from the synthesized compounds (Table 1). First, we found that replacement of the N-terminal β-Ala (compound 22, Table 1) with a γ-amino butyric acid (120H10, Table 1) seemed to favor binding

(position R1 in Table 1), while longer (123B1, Table 1) or bulkier substituents methylated on the alkyl chain were not tolerated (i.e comparing compounds 120G1 and 120G2, Table 1). At the C-terminus, replacement of the L-tryptophan of compound 120H10 with a tryptamine (123C2, Table 1) seemed well tolerated, while replacement of the indole ring with a naphthalene was not well tolerated (123C12, Table 1). Hence to further improve the activity of compound 123C2, we introduced a variety of substituents in the C-terminal tryptamine (compounds 123C3 to 123C7, Table 1). These studies resulted in the identification of compound 123C4 (Table 1, Fig. 1A) with Ki value in the FPA of 0.65 μM (Fig. 1B) and a dissociation constant for the EphA4-LBD of ~420 nM (Fig. 1C and Table 2).

Molecular basis for the affinity and the selectivity of 123C4 for the EphA4

To further assess the selectivity of 123C4, we tested it against the two most closely related receptors, namely the EphA3 (~ 73% sequence identity within the LBD) and the EphA2 (~ 55% sequence identity within the LBD). Under the same experimental conditions, 123C4 was inactive against the EphA2, while it displayed a Kd of approximately 4.5 μM against the EphA3 (Fig. 1 C), hence 123C4 was found to be ten-fold selective against the most closely related receptor, the EphA3. To further investigate at the molecular level the basis of binding and selectivity of 123C4 for the EphA4-LBD, we further employed NMR spectroscopy using uniformly ^{15}N-labeling or amino-acid selective ^{13}C-labeling, coupled with mutagenesis and molecular docking studies.

Docking studies with 123C4 and the X-ray structure of EphA4 in complex with ephrin-a5 (PDB ID 4M4R) (Xu et al., 2013) using the docking software Gold, (Cambridge Crystallographic Data Centre, UK) suggested several possible binding poses, owed to the flexibility of the ligand. To complicate the matter, the J-K loop in the EphA4 could adopt different conformations in the unbound and ligated forms (Singla et al., 2010). However, using the conformation of the EphA4 when bound to ephrin-a5, in one low energy binding pose (Fig. 1D), the ligand recapitulated several of the binding interactions produced by the binding loop from the ephrin ligand (Fig. 1E). In this pose, the backbone of 123C4 adopted a compact type I β-turn conformation, characterized by an intramolecular hydrogen bond between the carbonyl oxygen of the γ-aminobutyric acid and the amide hydrogen of the γ-pyridyl alanine residue, while the side chains made extensive contacts with the EphA4. As mentioned above, 123C4 showed a modest affinity for the EphA3-LBD, while it was inactive under the same experimental conditions against the EphA2-LBD (Table 2). Of note is that EphA4 and EphA3 differ by only few amino-acids in the region defined by ephrin binding site, most notably EphA4 residue Ile59 (Fig. 2A) that is a Glycine in EphA3. The X-ray structure of EphA3 has been recently reported (PDB ID 4LOP) (Forse et al., 2015) and superposition of EphA4 and EphA3 LBD confirmed that there are only few significant differences in the 123C4 ligand binding region between these proteins. Accordingly, single point mutation of Ile59 with an Alanine or a Glycine resulted in EphA4-LBD mutants with marked decreased in affinity for 123C4 as measured by ITC (Fig. 2B), with Kd values of 9 μM and 3.6 μM, respectively (Table 2). While docking studies may be largely inaccurate and only X-ray crystallographic data could ultimately confirm validity of the model, several experimental evidences suggested that the proposed binding pose of 123C4 in the EphA4 ephrin binding site may be plausible. For example, a salt bridge is anticipated between the

primary amino group of the γ-amino butyric acid moiety of 123C4 and the side chains of Asp61 and/or Glu62 (Fig. 2C). Accordingly, double mutation of these two residues resulted in an EphA4–LBD mutant that showed a 2 kcal/mol decrease in binding enthalpy for 123C4 (Table 2). Furthermore, in this binding pose the γ-amino butyric acid moiety would occupy a narrow channel formed by residues Ile59 and Met164, leaving limited space for larger substitutions in agreement with our SAR and selectivity data. Other single point mutations of selected binding site residues and the corresponding 123C4 binding data are reported in Table 2.

To further characterize the binding of 123C4 to EphA4-LBD we used NMR spectroscopy (Barile and Pellecchia, 2014; Pellecchia, 2005; Pellecchia et al., 2008; Pellecchia et al., 2002) monitoring chemical shift changes upon ligand titration. Notably, the changes in chemical shifts upon ligand titration occurred in slow-exchange in the NMR-time scale, typical of tight binding affinities (Barile and Pellecchia, 2014; Pellecchia, 2005; Pellecchia et al., 2008; Pellecchia et al., 2002) (Supplementary Fig. S1). Similarly, ligand titration with a selective $^{13}C^{\varepsilon}$-methionine labeled EphA4-LBD was carried out, and binding of 123C4 was monitored using 2D NMR [^{13}C,^{1}H] correlation spectra. Of the 5 Met residues present on the sequence of the EphA4-LBD, two are located in the ephrin binding site, namely Met164 and Met60 (Figs. 2C and 3A). The sequence specific resonance assignments of these two Met residues have been obtained by single point mutations followed by $^{13}C^{\varepsilon}$-methionine labeling and NMR analysis (Supplementary Fig. S2). Residue Met164 is particularly interesting as in the unbound, closed form of EphA4-LBD, partially fills a space that in the bound form is occupied by the ephrin ligand (Fig. 3A). Binding of the ephrin ligands caused a large conformational change in this region of the protein, resulting in the displacement of Met164 and opening of the binding site (Fig. 3A). Upon titration of 123C4, the cross-peaks corresponding to both $^{13}C^{\varepsilon}/^{1}H^{\varepsilon}$ of Met60 and Met164 progressively disappeared (Fig. 3B), while two new cross-peaks appeared, typical of binders in slow-exchange in the NMR-time scale (Pellecchia, 2005). Measuring the chemical shifts differences of cross-peaks in the free versus bound form, we estimated that an upper limit for the off rate for the complex, $k_{off} < 30\ s^{-1}$. Assuming a diffusion limited on rate of $10^9\ M^{-1}\ s^{-1}$, a dissociation constant Kd < 300 nM can be estimated, thus in close agreement with the FPA and ITC data. As controls, we also conducted similar titrations studies with the peptide KYL and with recombinant ephrin-B2 (Fig. 3B,C). In addition, we carried out NMR-based displacement assays using both [^{13}C,^{1}H] HSQC with $^{13}C^{\varepsilon}$ Met (Fig. 3C) labeled EphA4, and [^{15}N,^{1}H] correlation spectra with ^{15}N EphA4-LBD (supplementary Fig. S3) to assess the ability of 123C4 to compete with the ephrin-B2 for binding to the receptor. Binding of ephrin-B2 to EphA4 caused peak broadening in both spectra of the protein (Fig. 3C and supplementary Fig. S3). However in presence of 123C4 at 1:1:1 molar ratio with the EphA4 receptor and the ephrin-B2 ligand, the spectra of EphA4 more closely resembled those of the 123C4 bound form, indicating that under these experimental conditions (Fig. 3C and supplementary Fig. S3), 123C4 was able to displace the binding of ephrin-B2 to EphA4-LBD. Taken together, these data collectively strongly suggested that 123C4 is a potent and selective binder for EphA4-LBD that is capable of displacing the binding of the receptor for the ephrin-B2. The data gathered and the proposed binding pose may be used for eventual further refinements of the structure should these be needed at the development stage. Nonetheless we want to

emphasize again that proposed docking pose may still be largely inaccurate, given the large number of rotatable bonds in 123C4 and the flexibility of the loops of the EphA4-LBD forming the binding site. Currently we are hope to be able to obtain an experimentally derived structure, using X-ray crystallography, of the complex between 123C4 and the EphA4.

Cellular and in vivo efficacy studies in a mouse model of ALS

As mentioned, our working hypothesis was that elimination of both the N- and the C-termini of the peptide mimetics may result in molecules with increased drug-likeness, such as resistance to proteases and increased half-life and adsorption *in vivo* (supplementary Fig. S4). Using 1D ^{1}H NMR experiments in PBS, we determined that 123C4 has a solubility of about 100 μM, hence identifying PBS as a simple suitable formulation for delivery of the agent for further in cell and *in vivo* testing. Measurements of 123C4 stability in rat plasma indicated that the compound has a half-life $t_{1/2} > 60$ min (supplementary Fig. S4), hence significantly longer than the half-life of the KYL peptide ($t_{1/2} \sim 10$ min) measured under the same experimental conditions.

Further we measured the ability of our agents to affect EphA4 phosphorylation in cell cultures and to affect axon growth cone in primary cortical neuron cultures. Using primary hippocampal neurons, 123C4 appeared to stimulate the receptor. This is shown in Fig. 4A–E, where 123C4 displayed growth cone collapse activity, and induced EphA4 phosphorylation (**Fig. G–I**). These results suggested that 123C4 may activate the EphA4 receptor (Fig. 4F), in agreement with our binding and mutagenesis studies (see below). However, we want to report that when tested against a HEK293 cell line stably transfected with EphA4, 123C4 did not cause receptor phosphorylation, and antagonized the phosphorylation induced by ephrin-a5 (supplementary Fig. S7). This may be possibly due to several factors including cell size and over-expression of the receptor compared to other cellular components needed for endocytosis, for example. Hence, to further characterize the receptor internalization induced by 123C4 in primary cortical neurons, we prepared a fluorescently labeled version of the agent, namely FITC-123C4 (supplementary Fig. S6). Labeling the compound with a fluorescent tag allowed us to trace the endocytosis of 123C4 in primary neurons following its interaction with the EphA4 receptor. We found that at a concentration of 10 μM, FITC-123C4 was clearly detected within the cell. Moreover, the fluorescent compound co-localized with early endosomes, again suggesting that 123C4 may effectively induce EphA4 receptor endocytosis (Fig. 5). Notably, dose-dependent increase in the level of co-localization between FITC and an early endosomal marker EEA1 was observed in neurons treated with FITC-123C4 but not in neurons treated with FITC alone, indicating that specific endocytosis of 123C4 most likely occurred through its interaction with the EphA4 (Fig. 5). These data collectively suggested the 123C4 may act as an agonist for the EphA4 in primary cortical neurons.

Preliminary pharmacokinetics (PK) studies were conducted with a single dose of 123C4 (5 mg/Kg) administered intravenously in BalbC mice and compound concentration in blood and brain was measured after 30 minutes. Under these experimental conditions,

approximately 60% of the compound reached the brain, with concentrations similar to the Kd value of the compound for the EphA4-LBD (Supplementary Fig. S4).

Hence, because 5 mg/Kg established a dose that in principle is sufficient to inhibit the EphA4 in the brain, we decided to determine if this inhibition would result efficacious in mice models of ALS. First, to determine an approximate dose to be injected to SOD1(G93A)-mutant mice, 2 mice were initially treated postnatal day 60 until the endpoints with 30mg/Kg of 123C4 daily for several weeks intra-peritoneally and mice were observed for any signs of toxicity compared to untreated mice (n = 2) receiving only vehicle as control. At the end of the pilot study, no adverse sign of toxicity were observed in the treated mice compared to the control mice. In addition, increased survival was observed with the treated mice suggesting that a more robust study could be conducted with a more sizable number of animals.

Hence, equal number of SOD1(G93A)-mutant mice of the same gender from same litter were randomly divided into two groups (n = 12). Mice were treated from postnatal day 60 until the endpoints by i.p. injections with either 123C4 or the saline control. Daily treatment with 30 mg / kg of 123C4 improved average life span from 134.3 ± 7.2 days of control mice to 142.8 ± 6.9 days in 123C4-treated mice ($p < 0.01$, Student's t-test) while disease onset wasn't delayed. In addition, 123C4 treatment altered disease duration. The average survival time from disease onset to end point were 28.2 ± 4.2 and 38.6 ± 5.7 days ($p < 0.01$, Student's t-test) for control and 123C4-treated mice, respectively. Kaplan-Meier survival plots revealed an increased survival of 123C4-treated mice compared to control mice (Fig. 5H,I).

Discussion

EphA4 belongs to the Eph family of receptor tyrosine kinases, which together with their membrane-bound ligands, the ephrins (Eph receptor-interacting proteins), generate bi-directional signals controlling a multitude of cellular processes during development and in the adult (Pasquale, 2008). These receptors possess an extracellular ligand binding domain (LBD) that engages ephrin ligands and intracellular domains including a kinase domain, a sterile alpha motif (SAM) domain and PDZ binding motif that initiate the signal transduction cascade. While targeting the kinase domain is a possible avenue to inhibit a specific Eph receptor, obtaining selective ligands is notoriously challenging given the highly conserved ATP binding site of the kinase domain among these receptors and with other kinases. On the contrary, we and others reported that potent selective molecules can be obtained targeting the LBD. The critical roles of EphA4 in other physiological and pathological processes have been reported in recent studies validating EphA4 as a promising target for the development of small molecule drugs to treat several human diseases (Boyd et al., 2014), including abnormal blood clotting, spinal cord injury, and Alzheimer's disease (AD), in addition to amyotrophic lateral sclerosis.

Previous structural studies indicated that the EphA4-LBD contains a hydrophobic pocket surrounded by four flexible loops, which confer large structural plasticity to accommodate different binding partners (Bowden et al., 2009). Several 12-amino-acid-long peptide binders

that selectively block ephrin ligands from interacting with the EphA4 have been reported (Murai et al., 2003). For instance, the APY, KYL, and VTM peptides (which were named based on the first three amino acids of their sequences) bound to EphA4 tightly with Kd values in the low micromolar range (Lamberto et al., 2012; Murai et al., 2003). More recently a cyclic peptide was also reported but no indication on its resistance to proteases or brain penetration was reported (Lamberto et al., 2014). In addition, a few small molecular weight compounds that inhibit ephrin binding to EphA4 at low micromolar concentration have also been reported from HTS campaigns (Fu et al., 2014; Noberini et al., 2008). However, their detailed mechanism of action remains unclear and likely complex, possibly involving compound oxidation and/or non-specific binding, (Tognolini et al., 2014) which are typical issues encountered in traditional HTS hits (Baell and Holloway, 2010; Noberini et al., 2008). Indeed, two compounds reported to be EphA4-LBD binders, namely compound 1 (Noberini et al., 2008) and rhyncophilin (Fu et al., 2014), when tested in our NMR and ITC assays resulted inactive (Supplementary Fig. S5). Hence, while targeting the EphA4-LBD is possible in principle, HTS campaigns have thus far failed in producing viable pharmacological tools or lead compounds to validate EphA4 inhibition as therapeutic target for ALS and potentially other diseases (Tognolini et al., 2014).

Based on these observations, we used an innovative approach to drug discovery, termed HTS by NMR, that takes advantage of modern fragment based drug discovery principles (FBDD), combinatorial chemistry, and NMR-based screening to identify novel initial hit molecules and characterize their binding mode on the surface of the target (Barile and Pellecchia, 2014; Bottini et al., 2015; Wu et al., 2015a; Wu et al., 2013). Here, instead of testing by NMR mixtures of possible of fragments and subsequently synthesize bi-dentate agents after pairs of ligands have been discovered (Becattini and Pellecchia, 2006; Chen et al., 2007; Petros et al., 2010; Shuker et al., 1996), we combine the fragments directly into a common scaffold and test by NMR the pre-assembled molecules in mixtures gathered in positional scanning fashion (Wu et al., 2015a; Wu et al., 2013). These studies led to the identification of the initial hit molecule compound 22 (Table 1) that was able to bind selectively to the EphA4-LBD in the mid-micromolar range. Here we report on further SAR and iterative optimizations studies that led to compound 123C4, as potent and selective EphA4-LBD ligand (Figs. 1 and 2). At the molecular level, 123C4 was predicted to bind in the ephrin binding pocket possibly by placing its N-terminal γ-amino butyric acid in the deep, narrow, channel formed primarily by residues Ile59 and Met164 and ending with charged residues Asp61 and Glu62. Mutation of Ile59 with Ala or Gly (as present in the closely related EphA3-LBD) resulted in a dramatic reduction of binding affinity. Moreover, and again in agreement with such binding pose, introduction of bulkier residues at the N-terminus was detrimental for binding, owed to the anticipated tight fit between the γ–amino butyric acid moiety of 123C4 and the deep channel around Ile59. In addition, a possible salt-bridge between the N-terminal amino of 123C4 and the side chains of Asp61 and Glu62 is predicted by the binding pose and further corroborated by mutagenesis data (Table 2). Further, a dense network of additional favorable intermolecular interactions can be predicted by the proposed binding pose, involving for example the nitrogen atom in the pyridine ring, the oxygen atoms of both the tryptophan residue and the C-terminal tryptamine (Figs. 1D and 2C). 123C4 is more potent or equally potent than the reported linear or cyclic peptides,

albeit it has less than half the molecular weight of these agents, and it is more stable in plasma ($t_{1/2}$ > 60 min, supplementary Fig. S4) compared to the rapidly degraded peptides (for example, $t_{1/2}$ of KYL peptide in plasma is ~10 min). Preliminary *in vivo* PK studies in mice with this molecule revealed that the compound was capable to reach the brain at the evaluated time point and that chronic administration of the compound with repeated doses of the molecule in mice was well tolerated at the daily dose of 30 mg/kg for several weeks. We also found that two of recently reported HTS campaigns aimed at identifying EphA4-LBD inhibitors, resulted in compounds (namely compound 1 (Noberini et al., 2008) and rhyncophilin (Fu et al., 2014), supplementary Fig. S5) that did not appreciably interact with EphA4-LBD in our robust binding assays, underlining once again that traditional HTS screening methods are prone to selection of artifacts (Baell and Walters, 2014) and are not particularly suitable in deriving viable inhibitors of protein-protein interactions, albeit, if properly executed notable successful examples have been reported (Vassilev et al., 2004). Rather, in our experience and opinion targeting PPIs require a careful and iterative design of ligands, guided by robust and reproducible biophysical measurements (Barile and Pellecchia, 2014). Based on our studies, we are confident that we have developed a much needed novel, potent and selective pharmacological tool to interrogate the role of EphA4 in various disease models of neurodegeneration and cancer. To this point, most relevant are the recent genetic and animal model studies that clearly point at the EphA4 as a possible target for ALS (Van Hoecke et al., 2012), including demonstration that pharmacological inhibition of the EphA4 with the KYL peptide via an intra-cerebro-ventricular administration in ALS rats overexpressing human mutant SOD1 (G93A) prolonged survival (Van Hoecke et al., 2012). Hence, compound 123C4 in saline was injected daily intraperitoneally in SOD1(G93A) mice at a dose of 30 mg/kg. We chose this concentration based on the PK data obtained with 5mg/Kg indicating a brain concentration of about 100 nM after 30 minutes; of note is that ALS mice may have a leakier blood brain barrier (Bataveljic et al., 2014), hence even higher concentration of the drug may reach the brain in diseased animals. At this dose and regimen, compound 123C4 increased the average survival time from disease onset to end point and prolonged overall life span in SOD1(G93A) mice, similar to what observed in the *ephA4*$^{+/-}$ mice (Fig. 5H,I). As controls we used untreated mice receiving only the saline vehicle. While we contemplated using a similar yet inactive compound (i.e. compound 120G2) as negative control, we would have had to perform also a full PK, metabolism and toxicity analysis of such agent to make meaningful comparisons. Regarding 123C4, our data collectively indicated that the agent may act as an EphA4 agonist in primary cortical neurons, inducing receptor phosphorylation and endocytosis (Figs. 4, 5). To our knowledge this is the first EphA4 agonistic agent reported to date. Agonistic peptides and antibodies have been reported for the EphA2, an for these agents we and others have noticed that their agonistic could be enhanced by proper clustering the targeting agent in nanoparticles or synthesize dimers spaced by the appropriate linker (Duggineni et al., 2013). We are currently contemplating obtaining such dimeric or clustered 123C4 agents to further address this matter at the mechanistic level and to obtain perhaps even more potent agents.

To further characterize the binding of 123C4 to the EphA4, also in view of the observed agonist activity of the agent, we used a combination of computational modeling guided by NMR spectroscopy with selectively labeled EphA4-LBD, measurements of the

thermodynamics of binding, and mutagenesis. Recent X-ray crystallography studies with the EphA4 receptor in complex with an ephrin ligand suggested that ligand binding to the EphA4 receptor induces a conformational change in the JK loop in the EphA4-LBD that enables receptor dimerization (Xu et al., 2013). Hence, we used $^{13}C^{\varepsilon}$-Met labeled samples of EphA4 LBD to monitor and compare the binding of the antagonist peptide KYL, the agonist ephrin-B2, and 123C4. We chose Met residues because of the 5 met residues in our EphA4 LBD construct, Met60 is located in the ephrin binding site, while Met164 is located in the JK loop partially occupying the binding site in the unbound form (Figs. 2C and 3A). As mentioned, we found that the binding of 123C4 to EphA4-LBD was in slow exchange in the NMR time scale, again indicative of tight binding (Kd < 300 nM). Both KYL and 123C4 caused significant changes in the chemical shifts of both Met residues in 2D [^{13}C, ^{1}H] HSQC experiments, while the other Met residues were less affected. However, unlike KYL (an antagonistic peptide), 123C4 caused much larger changes in the chemical shifts of the $^{13}C^{\varepsilon}/^{1}H^{\varepsilon}$ resonances of the JK loop Met164, perhaps reflecting the conformational changes induced by 123C4 upon binding, that would agree with its agonistic activity. In agreement, ITC studies with 123C4 and a mutant Met164Ala EphA4-LBD revealed a similar enthalpy of binding of the compound for the mutant protein compared to wt-EphA4. However, binding of 123C4 to the Met164Ala mutant presented markedly reduced losses in entropy, compared to the binding to wt-EphA4, resulting in a dissociation constant of ~60 nM (Table 2), perhaps suggesting that the Met164Ala mutant did not need to undergo a large confirmation change to open the binding pocket to accommodate 123C4. Hence, our modeling data provided a reasonable framework to interpret SAR, NMR data, mutagenesis and binding affinities, and agonistic activity of 123C4. Clearly, these are computed models and as such may be largely inaccurate, hence detailed X-ray studies of the complex between EphA4 and 123C4 are being pursued.

Collectively our data suggested that 123C4 was able to bind to the EphA4 tightly and it was able to effectively compete with the natural ligand ephrin-B2. In addition, NMR studies suggested that the binding may be accompanied by conformational changes involving the JK loop, similar to what observed with the binding of natural agonists. Cellular studies with primary cortical neurons also suggested that the agent may act as an agonist, inducing receptor phosphorylation and endosomal internalization. Given these observations and the pro-survival effects exerted by 123C4 in mice models of ALS, it is tempting to speculate that perhaps is not the forward signaling of EphA4 activation that is correlated with the progression of ALS, but rather the reverse signaling induced by its ligand, ephrin-B2 in particular. Recent studies indeed attributed the expression of the ephrin-B2 ligand and signaling in astrocytes as critical in preventing the repair and regeneration of axons in a mouse model of spinal cord injury (Ren et al., 2013). Here, our data may likewise speculatively suggest that the ephrin-B2 may prevent the repair of damaged motor neurons in ALS. If these hypotheses are correct, the progression of ALS may be in part due to a neuro-inflammatory response mediated by ephrin-B2 rich astrocytes engaging EphA4 rich motor neurons. In this case, we anticipate that an EphA4 agonist may be more effective than an antagonist given that an agonist, as shown in Fig. 5, causes receptor internalization hence eliminating its possible engagement with ephrin-B2 rich astrocytes, therefore indirectly antagonizing reactive astrogliosis (Vargas and Johnson, 2010).

While future studies are needed to fully characterize the mechanism of action of these new class of compounds, we are confident that 123C4 is a powerful and unprecedented pharmacological tool to interrogate the complex cellular mechanisms that relates EphA4 signaling to the onset and progression of ALS and potentially other neurodegenerative diseases. The chemical structure of the compound and our characterization of binding and selectivity provide ample opportunities to guide eventual optimizations of this molecule should it become a necessary task at the development stage of the compound. Nonetheless, based on our preliminary *in vivo* efficacy studies, we are confident that such endeavors, combined with more detailed PK/PD studies, could guide the development of 123C4 or derivatives into an IND (Investigational New Drug), enabling human clinical trials for the treatment of ALS and potentially other human disorders.

Significance

Despite tremendous efforts no effective treatment is currently available for ALS, in spite of several clinical trials based on drugs from animal studies, which have been conducted and ultimately failed. Only recently, the EphA4 receptor has been identified as a disease modifying gene in animal models and in humans affected by the disease. However, no viable pharmacological agents are currently available that selectively target this gene to advance possible new therapies for ALS. Hence, we report on the design and characterization of a novel, potent and selective ligand targeting the EphA4 receptor that is very efficacious in delaying the progression of the disease in a mouse model of amyotrophic lateral sclerosis. The ALS protecting agent acts as an EphA4 agonist and not as antagonist, suggesting that the EphA4 mediated progression of motor neuron degeneration may be more complex than anticipated and may possibly involve reactive astrogliosis via the EphA4/ephrin-B2 interactions. Apart from these unprecedented results, the physicochemical nature of the selected agent, its pharmacological properties, and the observed efficacy in the mouse model of ALS, could support that this class of molecules may be provide an invaluable stepping stone for the development of innovative targeted therapies to delay the progression of ALS.

Experimental Procedures

General Synthesis

The synthetic scheme for the reported agents and details related to the synthetic schemes used are reported as supplementary Fig. S6. The final compounds were characterized by NMR and MALDI-Mass. All compounds were >95% purity.

Fluorescence Polarization Assays (FPAs)

The EphA4 binding KYL peptide (KYLPYWPVLSSL) (Murai et al., 2003) was labeled at the N-terminus with fluorescein isothiocyanate (FITC) and purified by HPLC. For competitive binding assays, 1 μL of 200 μM EphA4 LBD was pre-incubated with the tested compounds at various concentrations in 98 μL PBS (pH = 7.2) in 96-well black plates at room temperature for 10 min, and then 1 μL of 500 μM FITC labeled EphA4 peptide was added to produce a final volume of 100 μL. The KYL and DMSO were incubated in each assay as positive and negative controls, respectively. After 30 min of incubation at room

temperature, the polarization values in millipolarization units were measured at excitation/emission wavelengths of 480/535 nm with a multilabel plate reader (PerkinElmer, Waltham, MA, USA). K_i value was determined by fitting the experimental data to a Sigmoidal dose-response (variable slope) nonlinear regression model (GraphPad Prism version 5.01 for Windows, GraphPad Software, San Diego, CA, USA).

NMR spectroscopy

NMR spectra were acquired on 700 MHz Bruker Avance spectrometer equipped with TCI cryoprobe. All NMR data were processed and analyzed using TOPSPIN2.1 (Bruker Biospin Corp., Billerica, MA, USA) and SPARKY3.1 (University of California, San Francisco, CA, USA). 2D-[^{15}N, ^{1}H]-HSQC experiments were acquired using 32 scans with 2048 and 128 complex data points in the ^{1}H and ^{15}N dimensions at 300 K.

Protein-ligand interactions studies and molecular modeling

The purified EphA proteins (EphA4-LBD, EphA3-LBD and EphA2-LBD) were dissolved in 50 mM potassium phosphate buffer (pH 6.5), containing 100 mM NaCl. Compound binding was detected at 27 °C by comparing either the 2D-[^{15}N, ^{1}H]-HSQC or 2D-[^{13}C, ^{1}H]-HSQC spectra of 50 μM EphA4 LBD in absence and presence of compounds at 50 μM. ITC were measured with Model ITC200 from Microcal/GE Life Sciences. The selected docked conformation for the binding of 123C4 to the EphA4 LBD was obtained using Gold (Cambridge Crystallographic Data Centre; www.ccdc.cam.ac.uk) and the PDB ID 4M4R. Prior the docking, the protein and the ligands were prepared using Chimera (http://www.cgl.ucsf.edu/chimera) and SYBYL-X 1.2 (Tripos International, 1699 South Hanley Rd., St. Louis, Missouri, 63144, USA).

Primary neuron cultures

Primary cortical or hippocampal neurons were isolated from the brains of C57BL/6 mice at postnatal (P) 0-P1 or embryonic day (E) 18-E18, respectively. Tissues were dissected and treated with a papain/DNase I [0.1 M PBS/ 0.1% BSA/ 25mM glucose/ 5% papain/ 1X DNase I (Sigma, D5025-15K)] solution for 20 min at 37°C. Neurons were mechanically dissociated, plated on poly-D-lysine (0.5mg/ml) and laminin (5μg/ml) coated coverslips (50,000 cells per coverslip) or 6-well plates (330,000 per well) and maintained in Neurobasal media with 25 μM glutamine, 1% penicillin-streptomycin and B27 supplement (Invitrogen, 17504-044) under 5% CO_2/10% O_2 atmosphere at 37ºC.

Immunocytochemistry

Primary neurons were fixed with 4% PFA in 0.1 M PBS for 30 min at room temperature, then washed 3 x 10 min with 0.1 M PBS. Cells were permeabilized for 5 min at room temperature with 0.1% Triton X in 0.1 M PBS then washed 3 x 10 min in 0.1 M PBS. Cells were blocked with 5% BSA in 0.1 M PBS for an hour at room temperature. To visualize axon growth cones cells were stained with phalloidin-rhodamine (1:40, Invitrogen, R415) for an hour at room temperature and dendrites were immunolabeled with anti-MAP2 antibody (1:500, Sigma, M4403) in 0.1 M PBS containing 1% BSA for an additional 2 h at room temperature. Early endosomes were immunostained with rabbit anti-EEA1 (1:350,

Abcam, Ab2900) in 0.1 M PBS containing 1% BSA for overnight at 4°C. Coverslips were washed 3 x 10 min with 0.1 M PBS at room temperature followed by the incubation with Alexa Flour 594-conjugated donkey anti-mouse IgG (4 μg/ml; Molecular Probes) or Alexa Fluor 647-conjugated donkey anti-rabbit IgG (2 μg/ml; Thermo Fisher Scientific) for an hour at room temperature, respectively. Coverslips were mounted on slides with Vectashield mounting medium containing DAPI (Vector Laboratories Inc.) or with 0.1 M PBS.

Image analysis

For growth cone and endocytosis analysis, images were captured using a Nikon Eclipse TE2000-U inverted fluorescent microscope with a 20X air objective and a Hamamatsu ORCA-AG 12-bit CCD camera using Image-Pro software. High-resolution confocal images were captured with a Leica SP5 or Zeiss 510 confocal laser-scanning microscope using a series of high-resolution optical sections (1,024 x 1,024 format) with a 63 X objective at 1-μm step intervals (z-stack of 3 optical sections). For analysis, 100 images were collected (2–3 neurons/image) per treatment group. Axon was identified as a longest neurite of MAP-2 positive cells. Axon growth cones were assessed based on filamentous (F) actin labeling and classified into collapsed and growing based on their morphology. The percentage of neurons with collapsed axon growth cones was determined. Statistical differences for multiple groups were assessed by one-way ANOVA followed by Tukey post-hoc tests. Colocalization of FITC-123C4 or FITC (as a control) and EEA1 was determined by counting colocalized pixels per cell area (μm) using Colocalization Threshold plugin of ImageJ 2.0.0-rc-54. Statistical analysis was performed using two-tailed, unpaired student's *t* test.

Activation of EphA4 receptor

EphrinA1-Fc (R&D systems; 602-A1) and human Fc (R&D systems; 110-HG) were pre-clustered by the incubation with goat anti-human IgG (Jackson ImmunoResearch) for 1h at 4ºC. At 6 days *in vitro* (DIV) primary neurons were treated with pre-clustered Fc (2 μg/ml), ephrin-A1 (2 μg/ml), 500 nM 123C4, 5 μM 123C4, 10 μM 123C4 or 100 μM 123C4 for 30 min at 37°C under 5% CO_2/10% O_2 atmosphere and then processed for immunostaining or Western blotting. In all experiments, the concentration of DMSO is kept at 0.1 %. Cultures treated with 100 μM 123C4 plus ephrin-A1 were pre-treated with 100 μM 123C4 for 15 min then media was replaced with 100 μM 123C4/ephrin-A1 and incubated for an additional 15 min.

Western blot analysis

Cells were collected and lysed in the lysis buffer (25 mM Tris-HCl, 150mM NaCl, 5mM EDTA, 1% Triton-X, 1mM sodium pervanadate and protease inhibitor cocktail (1:100, Sigma, P8340)) at 4°C for 30 min. Cell lysates were cleared by centrifugation at 13,500rpm for 15min at 4°C, then incubated with protein-A agarose beads (Sigma, P1406) and anti-EphA4 antibody (Invitrogen, 371600), for 2hrs at 4°C. Beads were boiled in reducing sample buffer (Laemmli 2X concentrate, Sigma, S3401). Samples were briefly spun down and the supernatant was run on an 8–16% Tris-glycine SDS-PAGE precast gels (Life Technologies, EC6045BOX). Proteins were transferred onto a Protran BA 85 Nitrocellulose membrane (GE Healthcare) and blocked for 1 h at room temperature in 5% BSA. The blots were incubated with HRP-conjugated anti-phosphotyrosine antibody (BD Transduction,

610000) in TBS/0.1% Tween-20/5% BSA at 4°C overnight and developed with ECL Detection reagent (Thermo Scientific, #80196). For re-probing, membrane blots were washed in stripping buffer (2% SDS, 100 mM β-mercaptoethanol, 50 mM Tris-HCl, pH=6.8) for 30 min at 56°C, and then washed 5 X 10 min with TBS, blocked with 5% skim milk, and then re-probed for EphA4 (Invitrogen, 371600). Blots were washed 3 x 10 min with TBS/0.1% tween-20 then incubated with α-mouse-HRP-conjugated secondary antibodies in TBS/0.1% tween-20/5% BSA (1:5000, GE Healthcare) for an hour at room temperature. After the incubation blots were washed 3 x 10 min with TBS/0.1% tween-20 and developed with ECL Detection reagent (Thermo Scientific, #80196). Developed films were then scanned and protein levels quantified by measuring band density values using ImageJ.

Animal studies

Equal number of SOD1(G93A)-mutant mice of the same gender from same litter were randomly divided into two groups. Littermates with same gender were randomly assigned to each group which had 12 mice (6 male and 6 female). The strain of the mutant SOD1(G93A) mice is B6.Cg-Tg(SOD1G93A)1Gur/J (Jackson Laboratory). The mice purchased from Jackson were not used immediately. The SOD1(G93A) male from Jackson mated with wild-type C57Bl/6 female, then male offspring were always mated with wild-type C57Bl/6 female mice. The resulting animals are on a background that involves C57BL/6 and SJL and express high levels of human SOD1 gene carrying a glycine to alanine transition at position 93 (G93A). The animal protocol used was approved by the Animal Welfare Committee of the Sanford Burnham Prebys Medical Discovery Institute. Mice were treated from postnatal day 60 until the endpoints by *i.p.* injections with either 123C4 or the saline control. 123C4 was dissolved in normal saline at a concentration of 2 mg/mL and sterilized by a 0.2 μm filter. Mice were treated with 123C4 every day, at a dose of 30 mg/kg of body weight. Animals were assessed daily for the time of onset of hind limb tremor and loss of splay reflex. The endpoint was designated as the point when the mouse could no longer roll over within 10s after being pushed onto its side. At this stage, mice were killed. Disease onset and survival time were compared using the Kaplan–Meier method. Difference of survival time from disease onset to end point between 123C4 and saline-treated mice was analyzed with Student's t-test. Values are given as mean ± SD. Preliminary BBB penetration and PK studies were performed by Agilux (Cambridge, MA).

Supplementary Material

Refer to Web version on PubMed Central for supplementary material.

Acknowledgments

This work was supported in part by NIH grants CA138390 and CA168517 to MP, and by a UCR Collaborative Seed Grant (to MP and IE). MP holds the Daniel Hays Chair in Cancer Research at the School of Medicine at UCR. Molecular graphics and analyses were performed with the UCSF Chimera package (http://www.cgl.ucsf.edu/chimera). Chimera is developed by the Resource for Biocomputing, Visualization, and Informatics at the University of California, San Francisco (supported by NIGMS P41-GM103311). We also thank the Sanford-Burnham-Prebys Medical Discovery Institute Protein Analysis Facility supported by NIH grant CA030199 for support with ITC measurements.

References

Baell J, Walters MA. 2014; Chemistry: Chemical con artists foil drug discovery. Nature. 513:481–483. [PubMed: 25254460]

Baell JB, Holloway GA. 2010; New substructure filters for removal of pan assay interference compounds (PAINS) from screening libraries and for their exclusion in bioassays. Journal of medicinal chemistry. 53:2719–2740. [PubMed: 20131845]

Barile E, Pellecchia M. 2014; NMR-based approaches for the identification and optimization of inhibitors of protein-protein interactions. Chem Rev. 114:4749–4763. [PubMed: 24712885]

Bataveljic D, Milosevic M, Radenovic L, Andjus P. 2014; Novel molecular biomarkers at the blood-brain barrier in ALS. Biomed Res Int. 2014:907545. [PubMed: 24949481]

Becattini B, Pellecchia M. 2006; SAR by ILOEs: an NMR-based approach to reverse chemical genetics. Chemistry. 12:2658–2662. [PubMed: 16121405]

Bottini A, Wu B, Barile E, De SK, Leone M, Pellecchia M. 2015High-Throughput Screening (HTS) by NMR Guided Identification of Novel Agents Targeting the Protein Docking Domain of YopH. ChemMedChem.

Bowden TA, Aricescu AR, Nettleship JE, Siebold C, Rahman-Huq N, Owens RJ, Stuart DI, Jones EY. 2009; Structural plasticity of eph receptor A4 facilitates cross-class ephrin signaling. Structure. 17:1386–1397. [PubMed: 19836338]

Boyd AW, Bartlett PF, Lackmann M. 2014; Therapeutic targeting of EPH receptors and their ligands. Nat Rev Drug Discov. 13:39–62. [PubMed: 24378802]

Chen J, Zhang Z, Stebbins JL, Zhang X, Hoffman R, Moore A, Pellecchia M. 2007; A fragment-based approach for the discovery of isoform-specific p38alpha inhibitors. ACS Chem Biol. 2:329–336. [PubMed: 17465519]

DeJesus-Hernandez M, Mackenzie IR, Boeve BF, Boxer AL, Baker M, Rutherford NJ, Nicholson AM, Finch NA, Flynn H, Adamson J, et al. 2011; Expanded GGGGCC hexanucleotide repeat in noncoding region of C9ORF72 causes chromosome 9p-linked FTD and ALS. Neuron. 72:245–256. [PubMed: 21944778]

Duggineni S, Mitra S, Lamberto I, Han X, Xu Y, An J, Pasquale EB, Huang Z. 2013; Design and Synthesis of Potent Bivalent Peptide Agonists Targeting the EphA2 Receptor. ACS Med Chem Lett. 4

Forse GJ, Uson ML, Nasertorabi F, Kolatkar A, Lamberto I, Pasquale EB, Kuhn P. 2015; Distinctive Structure of the EphA3/Ephrin-A5 Complex Reveals a Dual Mode of Eph Receptor Interaction for Ephrin-A5. PLoS One. 10:e0127081. [PubMed: 25993310]

Frugier T, Conquest A, McLean C, Currie P, Moses D, Goldshmit Y. 2012; Expression and activation of EphA4 in the human brain after traumatic injury. J Neuropathol Exp Neurol. 71:242–250. [PubMed: 22318127]

Fu AK, Hung KW, Huang H, Gu S, Shen Y, Cheng EY, Ip FC, Huang X, Fu WY, Ip NY. 2014; Blockade of EphA4 signaling ameliorates hippocampal synaptic dysfunctions in mouse models of Alzheimer's disease. Proc Natl Acad Sci U S A. 111:9959–9964. [PubMed: 24958880]

Fukai J, Yokote H, Yamanaka R, Arao T, Nishio K, Itakura T. 2008; EphA4 promotes cell proliferation and migration through a novel EphA4-FGFR1 signaling pathway in the human glioma U251 cell line. Mol Cancer Ther. 7:2768–2778. [PubMed: 18790757]

Goldshmit Y, Galea MP, Wise G, Bartlett PF, Turnley AM. 2004; Axonal regeneration and lack of astrocytic gliosis in EphA4-deficient mice. The Journal of neuroscience : the official journal of the Society for Neuroscience. 24:10064–10073. [PubMed: 15537875]

Hanell A, Clausen F, Djupsjo A, Vallstedt A, Patra K, Israelsson C, Larhammar M, Bjork M, Paixao S, Kullander K, et al. 2012; Functional and histological outcome after focal traumatic brain injury is not improved in conditional EphA4 knockout mice. J Neurotrauma. 29:2660–2671. [PubMed: 22985250]

Iiizumi M, Hosokawa M, Takehara A, Chung S, Nakamura T, Katagiri T, Eguchi H, Ohigashi H, Ishikawa O, Nakamura Y, et al. 2006; EphA4 receptor, overexpressed in pancreatic ductal adenocarcinoma, promotes cancer cell growth. Cancer Sci. 97:1211–1216. [PubMed: 16965393]

Lamberto I, Lechtenberg BC, Olson EJ, Mace PD, Dawson PE, Riedl SJ, Pasquale EB. 2014; Development and structural analysis of a nanomolar cyclic peptide antagonist for the EphA4 receptor. ACS Chem Biol. 9:2787–2795. [PubMed: 25268696]

Lamberto I, Qin H, Noberini R, Premkumar L, Bourgin C, Riedl SJ, Song J, Pasquale EB. 2012; Distinctive binding of three antagonistic peptides to the ephrin-binding pocket of the EphA4 receptor. The Biochemical journal. 445:47–56. [PubMed: 22489865]

Lemmens R, Van Hoecke A, Hersmus N, Geelen V, D'Hollander I, Thijs V, Van Den Bosch L, Carmeliet P, Robberecht W. 2007; Overexpression of mutant superoxide dismutase 1 causes a motor axonopathy in the zebrafish. Human molecular genetics. 16:2359–2365. [PubMed: 17636250]

Miyazaki K, Inokuchi M, Takagi Y, Kato K, Kojima K, Sugihara K. 2013; EphA4 is a prognostic factor in gastric cancer. BMC Clin Pathol. 13:19. [PubMed: 23738943]

Murai KK, Nguyen LN, Koolpe M, McLennan R, Krull CE, Pasquale EB. 2003; Targeting the EphA4 receptor in the nervous system with biologically active peptides. Molecular and cellular neurosciences. 24:1000–1011. [PubMed: 14697664]

Noberini R, Koolpe M, Peddibhotla S, Dahl R, Su Y, Cosford ND, Roth GP, Pasquale EB. 2008; Small molecules can selectively inhibit ephrin binding to the EphA4 and EphA2 receptors. The Journal of biological chemistry. 283:29461–29472. [PubMed: 18728010]

Oshima T, Akaike M, Yoshihara K, Shiozawa M, Yamamoto N, Sato T, Akihito N, Nagano Y, Fujii S, Kunisaki C, et al. 2008; Overexpression of EphA4 gene and reduced expression of EphB2 gene correlates with liver metastasis in colorectal cancer. Int J Oncol. 33:573–577. [PubMed: 18695888]

Pasquale EB. 2008; Eph-ephrin bidirectional signaling in physiology and disease. Cell. 133:38–52. [PubMed: 18394988]

Pellecchia M. 2005; Solution nuclear magnetic resonance spectroscopy techniques for probing intermolecular interactions. Chemistry & biology. 12:961–971. [PubMed: 16183020]

Pellecchia M, Bertini I, Cowburn D, Dalvit C, Giralt E, Jahnke W, James TL, Homans SW, Kessler H, Luchinat C, et al. 2008; Perspectives on NMR in drug discovery: a technique comes of age. Nat Rev Drug Discov. 7:738–745. [PubMed: 19172689]

Pellecchia M, Sem DS, Wuthrich K. 2002; NMR in drug discovery. Nat Rev Drug Discov. 1:211–219. [PubMed: 12120505]

Petros AM, Huth JR, Oost T, Park CM, Ding H, Wang X, Zhang H, Nimmer P, Mendoza R, Sun C, et al. 2010; Discovery of a potent and selective Bcl-2 inhibitor using SAR by NMR. Bioorg Med Chem Lett. 20:6587–6591. [PubMed: 20870405]

Ren Z, Chen X, Yang J, Kress BT, Tong J, Liu H, Takano T, Zhao Y, Nedergaard M. 2013; Improved axonal regeneration after spinal cord injury in mice with conditional deletion of ephrin B2 under the GFAP promoter. Neuroscience. 241:89–99. [PubMed: 23518227]

Rosen DR, Siddique T, Patterson D, Figlewicz DA, Sapp P, Hentati A, Donaldson D, Goto J, O'Regan JP, Deng HX, et al. 1993; Mutations in Cu/Zn superoxide dismutase gene are associated with familial amyotrophic lateral sclerosis. Nature. 362:59–62. [PubMed: 8446170]

Shuker SB, Hajduk PJ, Meadows RP, Fesik SW. 1996; Discovering high-affinity ligands for proteins: SAR by NMR. Science. 274:1531–1534. [PubMed: 8929414]

Singla N, Goldgur Y, Xu K, Paavilainen S, Nikolov DB, Himanen JP. 2010; Crystal structure of the ligand-binding domain of the promiscuous EphA4 receptor reveals two distinct conformations. Biochem Biophys Res Commun. 399:555–559. [PubMed: 20678482]

Spanevello MD, Tajouri SI, Mirciov C, Kurniawan N, Pearse MJ, Fabri LJ, Owczarek CM, Hardy MP, Bradford RA, Ramunno ML, et al. 2013; Acute delivery of EphA4-Fc improves functional recovery after contusive spinal cord injury in rats. J Neurotrauma. 30:1023–1034. [PubMed: 23557244]

Tognolini M, Incerti M, Lodola A. 2014; Are we using the right pharmacological tools to target EphA4? ACS Chem Neurosci. 5:1146–1147. [PubMed: 25405504]

Van Hoecke A, Schoonaert L, Lemmens R, Timmers M, Staats KA, Laird AS, Peeters E, Philips T, Goris A, Dubois B, et al. 2012; EPHA4 is a disease modifier of amyotrophic lateral sclerosis in animal models and in humans. Nature medicine. 18:1418–1422.

Vargas MR, Johnson JA. 2010; Astrogliosis in amyotrophic lateral sclerosis: role and therapeutic potential of astrocytes. Neurotherapeutics. 7:471–481. [PubMed: 20880509]

Vassilev LT, Vu BT, Graves B, Carvajal D, Podlaski F, Filipovic Z, Kong N, Kammlott U, Lukacs C, Klein C, et al. 2004; In vivo activation of the p53 pathway by small-molecule antagonists of MDM2. Science. 303:844–848. [PubMed: 14704432]

Wu B, Barile E, De SK, Wei J, Purves A, Pellecchia M. 2015a; High-Throughput Screening by Nuclear Magnetic Resonance (HTS by NMR) for the Identification of PPIs Antagonists. Curr Top Med Chem. 15:2032–2042. [PubMed: 25986689]

Wu B, Wang S, De SK, Barile E, Quinn BA, Zharkikh I, Purves A, Stebbins JL, Oshima RG, Fisher PB, et al. 2015b; Design and Characterization of Novel EphA2 Agonists for Targeted Delivery of Chemotherapy to Cancer Cells. Chemistry & biology. 22:876–887. [PubMed: 26165155]

Wu B, Zhang Z, Noberini R, Barile E, Giulianotti M, Pinilla C, Houghten RA, Pasquale EB, Pellecchia M. 2013; HTS by NMR of combinatorial libraries: a fragment-based approach to ligand discovery. Chemistry & biology. 20:19–33. [PubMed: 23352136]

Xu K, Tzvetkova-Robev D, Xu Y, Goldgur Y, Chan YP, Himanen JP, Nikolov DB. 2013; Insights into Eph receptor tyrosine kinase activation from crystal structures of the EphA4 ectodomain and its complex with ephrin-A5. Proc Natl Acad Sci U S A. 110:14634–14639. [PubMed: 23959867]

Highlights

- We report a novel, potent and selective ligand targeting the EphA4 receptor.
- Binding of the ligand is selective and enthalpy driven as verified by ITC
- The agent acts as an EphA4 agonist in primary neurons
- The agent is very efficacious in delaying the progression of ALS in mouse a model

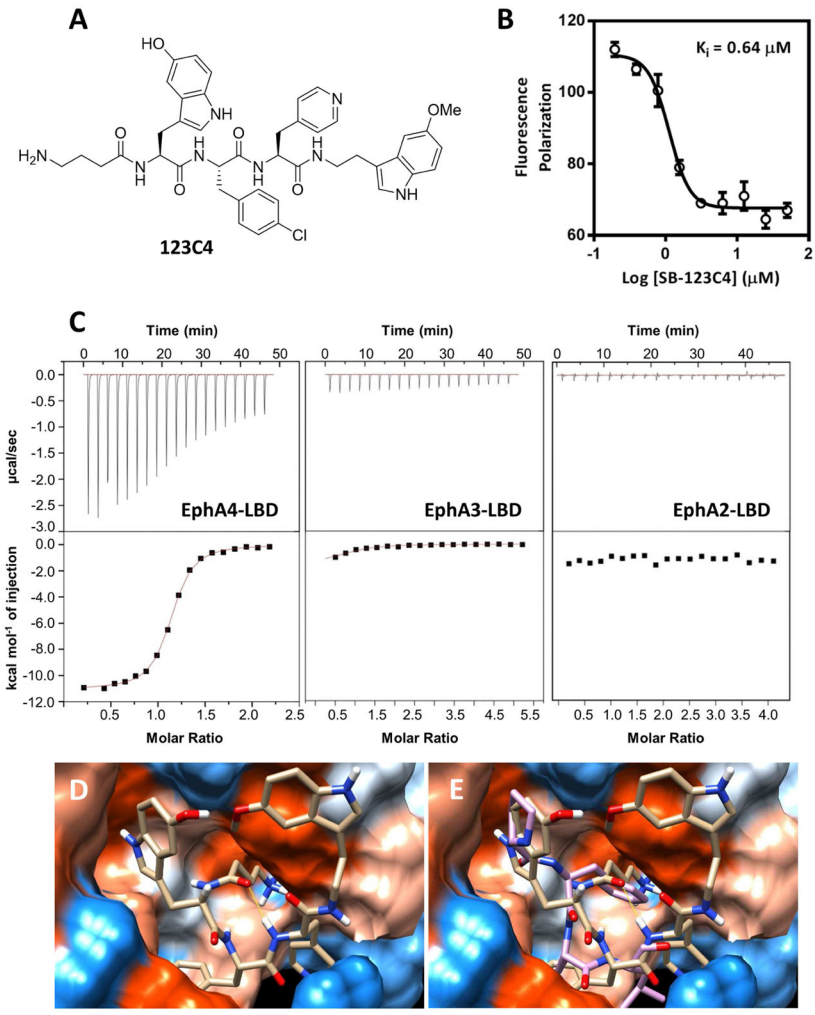

Fig. 1. Binding and selectivity data for compound 123C4

A) Chemical structure of 123C4. **B)** Dose response curve for 123C4. The binding of 123C4 to EphA4 LBD was monitored by measuring the changes in anisotropy as it displaced the known binding peptide KYL from the active site. **C)** ITC binding curves of 123C4 to EphA4, EphA3 and EphA2 LBDs. **D)** Docked models of 123C4 in the ephrin binding site of EphA4 (PDB ID 4M4R). The compound can adopt a type I β-turn, stabilized by an intramolecular hydrogen bond (indicated in yellow) between the carbonyl of the first residue of the turn (ψ-amino butyric acid) and the amide hydrogen of the fourth residue of the turn (ψ=pyridyl alanine). **E**) Superposition of the docked structure of 123C4 as in **D**) with the portion of the ephrin ligand loop of sequence ^{123}ProPheSerLeu^{126} (from PDB ID 4M4R) that occupies the EphA4 LBD binding pocket. The models were obtained as described in the methods section and the structural figures were generated using Chimera (http://www.cgl.ucsf.edu/chimera).

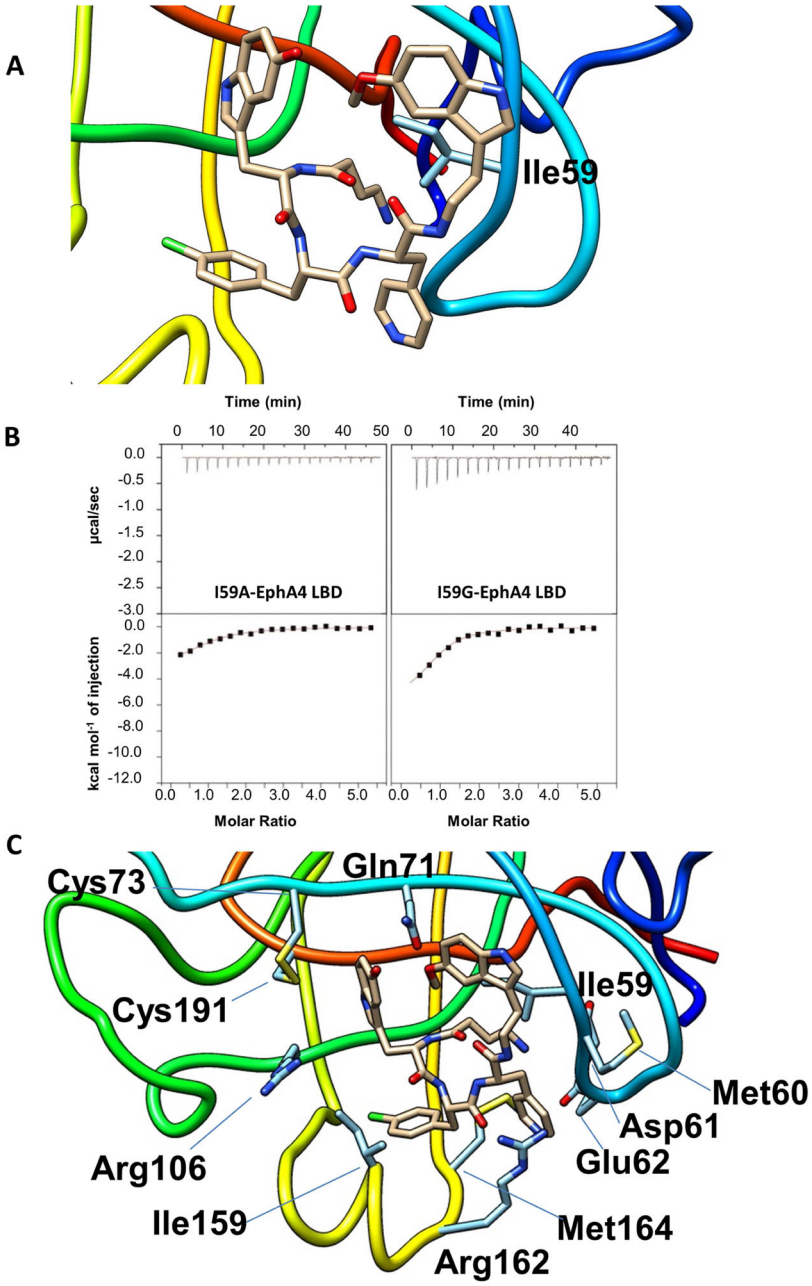

Fig. 2. Molecular basis for the selectivity and activity of 123C4

A) Isothermal titration calorimetry curves for the binding of 123C4 to EphA4 mutants. **B**) Docked structure of 123C4 in complex with EphA4 LBD (using the structure of EphA4 in complex with an ephrin ligand, PDB ID 4M4R), highlighting the side chain of Ile59. **C**) Docked structure of 123C4 in complex with EphA4 LBD (as in **C**) highlighting several of the side chains of residues in direct contact with the ligand.

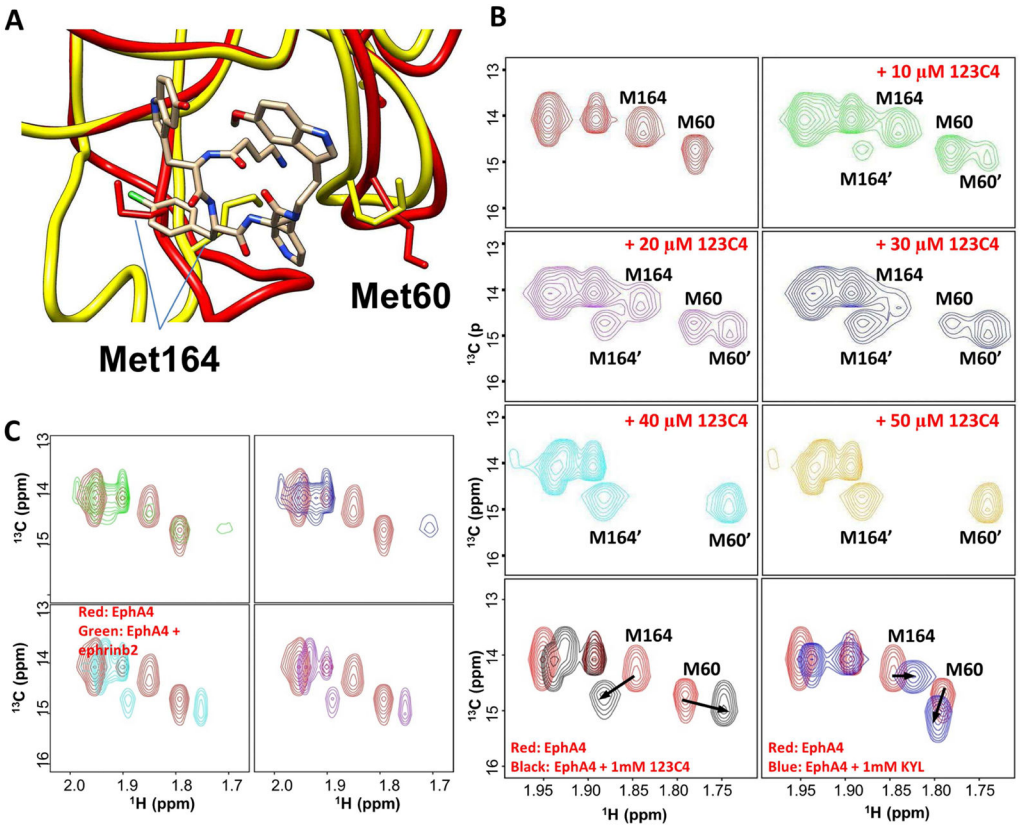

Fig. 3. NMR binding studies with 123C4 and ^{13}C Met labeled EphA4 LBD

A) 2D [^{13}C, ^{1}H]-HSQC spectra of 50 μM ^{13}C$^{\varepsilon}$-Methionine labeled EphA4 LBD in the absence and presence of 123C4 at different ligand concentrations. The spectra collected in presence of DMSO (control), 10 μM, 20 μM, 30 μM, 40 μM and 50 μM 123C4 were colored in red, green, purple, blue, cyan and yellow, respectively. Bottom two are overlays of [^{13}C, ^{1}H]-HSQC spectra of 50 μM ^{13}C-Met labeled EphA4 LBD in the absence and presence of 1 mM 123C4 (black) and KYL peptide (blue). **B)** Overlays of [^{13}C, ^{1}H]-HSQC spectra of 10 μM ^{13}C-Met labeled EphA4 LBD in the absence (red) and presence of 10 μM ephrin-B2 (green), 20 μM ephrin-B2 (blue), 20 μM ephrin-B2 plus 20 μM 123C4 (cyan) and 20 μM ephrin-B2 plus 40 μM 123C4 (purple). The resonance assignments for binding sites Met60 and Met164 are indicated. **C**) Docked structure of 123C4 in complex with EphA4 LBD in its ephrin-ligand bound form (yellow; PDB ID 4M4R) is overlaid to the EphA4 LBD in its unbound form (red; PDB ID 4BK4). The side chains of residues Met61 and Met 164 are shown.

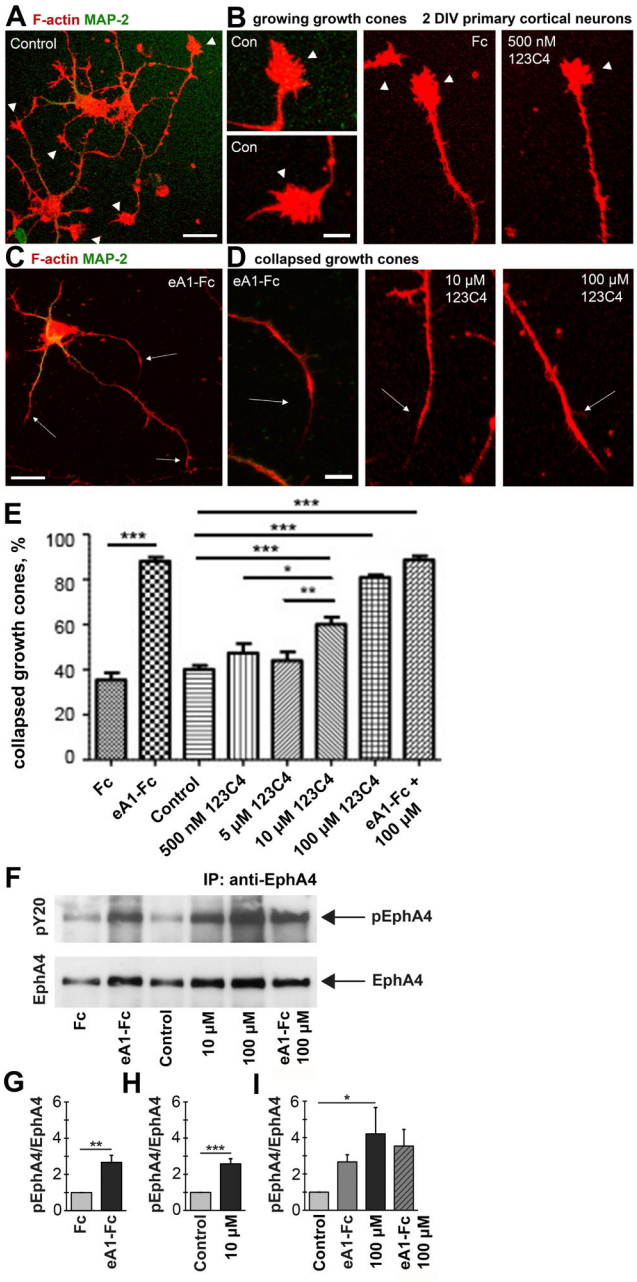

Fig. 4. Compound 123C4 induces growth cone collapse and EphA4 phosphorylation in primary cortical neuron cultures

Confocal images of 2 DIV primary cortical neurons untreated (control), treated with Fc (Fc), ephrinA1-Fc (ephrinA1-Fc), 500 nM 123C4, 10 μM 123C4 and 100 μM123C4. Axon growth cone morphology was assessed by labeling for F-actin with rhodamine-coupled phalloidin (red). Neurons were identified by immunostaining against MAP-2 (green). (**B,D**) High magnification images of growing (**B**) and collapsed (**D**) growth cones. Scale bars are 20 μm in A, C and 5 μm in B, D. (**E**) Graph shows average percent of collapsed growth cones in primary cortical neuron cultures untreated (control), treated with Fc (Fc), ephrinA1-Fc (ephrinA1-Fc), 500 nM 123C4, 5 μM 123C4, 10 μM 123C4, 100 μM 123C4, or 100 μM

123C4 plus ephrinA1-Fc. Error bar indicates SEM (n=100–200 neurons per group; experiment was repeated three times). Statistical analysis was performed using two-way ANOVA followed by Tukey's post-hoc analysis (*p < 0.05, **p < 0.01, ***p < 0.001). (**F–I**) Compound 123C4 induces EphA4 phosphorylation in primary neurons. **(F)** Western blot analysis of pEphA4 (upper panel) and total EphA4 (lower panel) in cultures of primary neurons untreated (control), treated with Fc (Fc), ephrin A1-Fc (eA1-Fc), 10 μM 123C4, 100 μM 123C4, and 100 μM 123C4 plus ephrin A1-Fc for 30 min. **(G–I)** Graphs showing average ratio of pEphA4 and total EphA4 in primary neuron cultures treated with Fc (Fc) and ephrin A1-Fc (ephrin A1-Fc) **(G)**; untreated (control), and 10 μM 123C4 **(H)**; untreated (control), ephrin A1-Fc, 100 μM 123C4 or 100 μM 123C4 plus ephrin A1-Fc **(I)**. Error bars indicate SEM (the experiment was repeated four times). Statistical analysis was performed using two-tailed, unpaired student's *t* test for comparison of two groups; **p < 0.01 (p=0,00264), ***p < 0.001 (p=0,000653) **(F–G)** or two-way ANOVA followed by Bonferroni's post-hoc analysis (*p < 0.05) **(I)**.

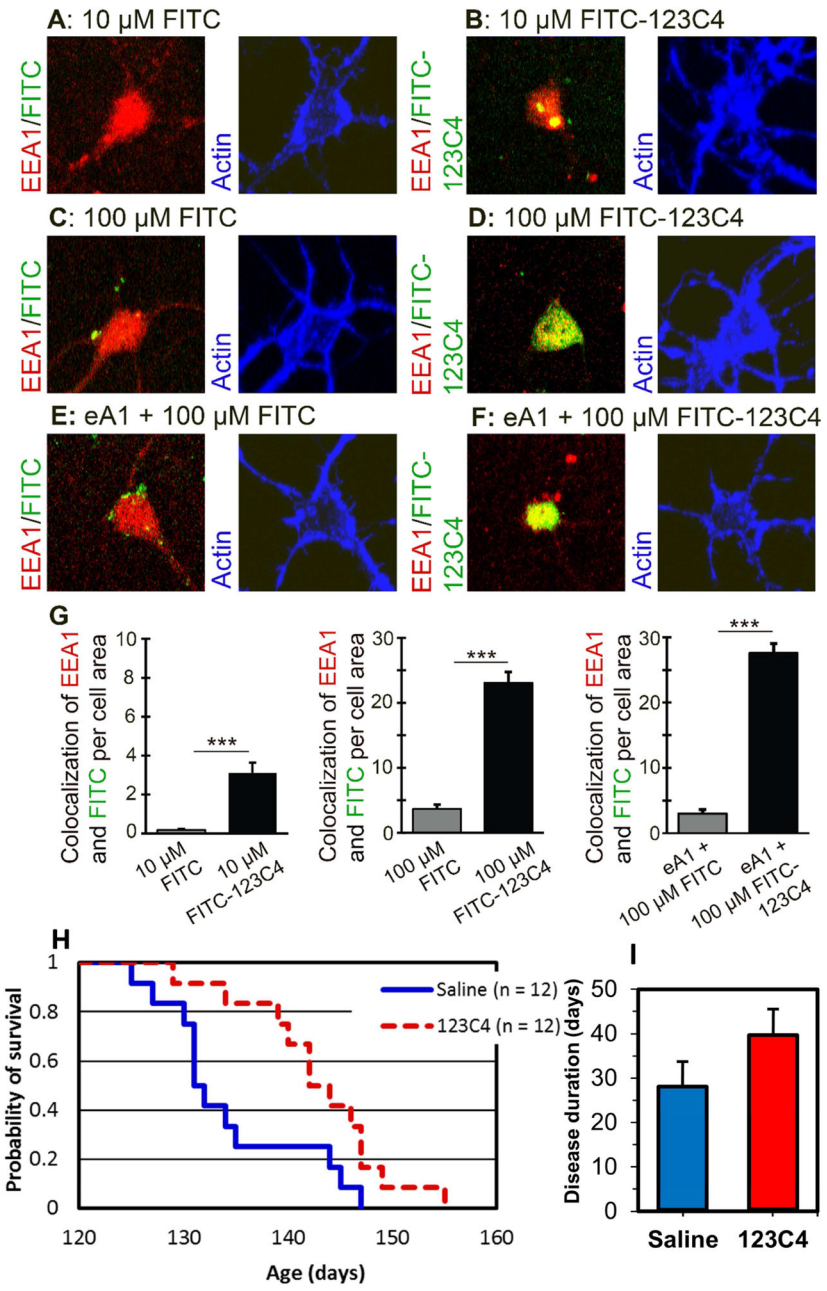

Fig. 5. Endocytosis of FITC-labeled compound 123C4 by primary neurons in cultures *and in vivo* efficacy in an ALS mouse model

(A–F) Confocal images of 6 DIV primary neurons treated with 10 μM FITC **(A)**, 10 μM FITC-123C4 **(B)**, 100 μM FITC **(C),** 100 μM FITC-123C4 **(D)**, 100 μM FITC plus ephrin A1-Fc **(F),** or 100 μM FITC plus ephrin A1-Fc **(E).** Neurons were labeled for F-actin with rhodamine-coupled phalloidin (blue) and endosomes were identified by immunostaining against early endosome marker EEA1 (red). **(G)** Colocalization of FITC-123C4 or FITC and EEA1 per cell area (pixel per μm) was measured using ImageJ 2.0.0-rc-54. Graphs show average values and error bars indicate SEM (n=25–35 neurons per group). Statistical analysis was performed using two-tailed, unpaired student's *t* test (***p < 0.001). **(H,I)**. *In*

vivo efficacy studies with 123C4. (**H**) Cumulative probabilities of survival time of SOD1(G93A) mice treated with 123C4 (in saline, 30 mg/Kg, i.p. daily) or saline alone. 123C4 treatment prolonged survival without affecting the disease onset. (**I)** Treatment with compound 123C4 increased the average survival time from disease onset to end point and prolonged overall life span in SOD1(G93A) mice, similar to what observed in the *ephA4 +/−* mice. The data were analyzed using the Kaplan–Meier method.

Table 1

Structure Activity Relationships (SAR) studies for EphA4-LBD ligands.

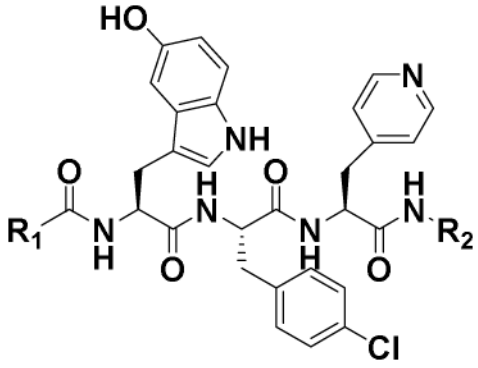

ID	R_1	R_2	K_i (μM) by FPA	K_d (μM) by ITC
compound 22	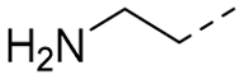	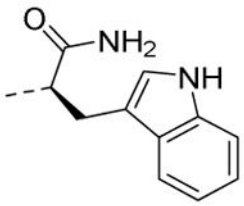	2.14	1.2
120H10		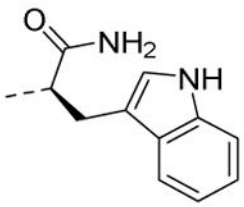	0.96	ND
123B1		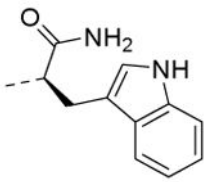	3.04	ND
120G1	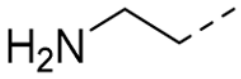	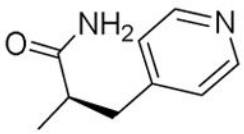	13.96	ND

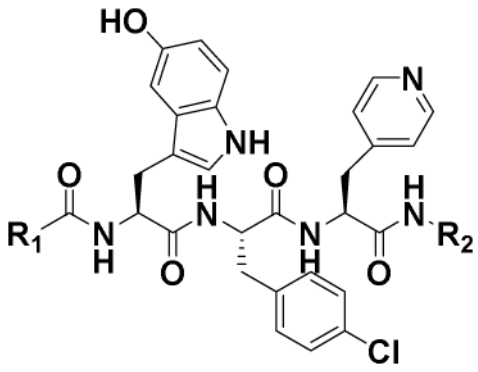

ID	R_1	R_2	K_i (μM) by FPA	K_d (μM) by ITC
120G2		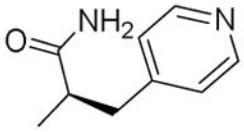	>100	ND
123C2		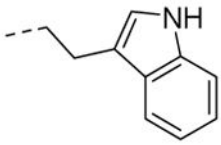	1.59	1.1
123C12		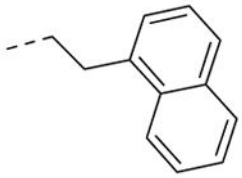	7.67	ND
123C3		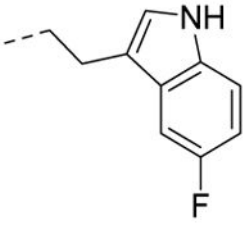	2.22	ND
123C5		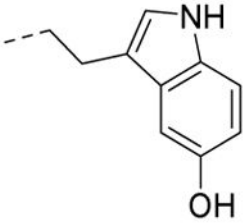	2.57	2.2

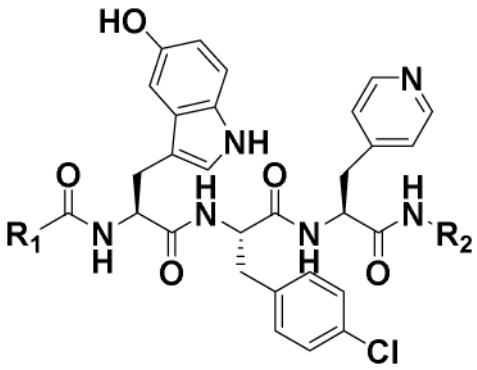

ID	R_1	R_2	K_i (μM) by FPA	K_d (μM) by ITC
123C6		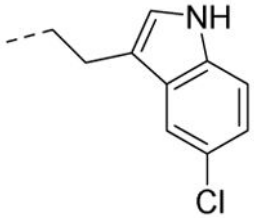	3.14	ND
123C7		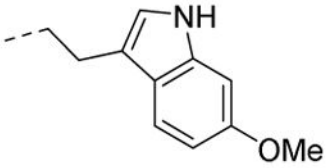	1.59	0.54
123C4		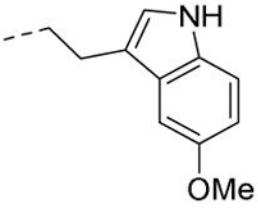	0.64	0.42

Table 2

Thermodynamic parameters for binding of 123C4 to various EphA4-LBD mutants, EphA3-LBD, and EphA2-LBD. N.B. = no binding.

Protein	K_d (μM)	ΔH (kcal/mol)	TΔS (kcal/mol)
wt-EphA4 LBD	0.42 ± 0.02	−11.06 ± 0.06	−2.42
wt-EphA3 LBD	4.55 ± 1.09	−1.54 ± 0.30	5.75
wt-EphA2 LBD	N.B.	-	-
I59G-EphA4 LBD	3.66 ± 0.71	−5.69 ± 0.74	1.68
I59A-EphA4 LBD	9.09 ± 1.49	−3.43 ± 0.41	3.43
I67A-EphA4 LBD	0.78 ± 0.08	−4.54 ± 0.08	3.75
I159A-EphA4 LBD	0.29 ± 0.02	−8.53 ± 0.06	0.34
M60A-EphA4 LBD	0.35 ± 0.03	−9.98 ± 0.21	−1.24
M164A-EphA4 LBD	0.062 ± 0.01	−11.14 ± 0.13	−1.38
D61G/E62G-EphA4 LBD	0.34 ± 0.04	−9.13 ± 0.14	−0.37